Int J Clin Exp Med 2014;7(12):4747-4758
www.ijcem.com /ISSN:1940-5901/IJCEM0002728

Original Article

Targeted fluorescent magnetic nanoparticles for imaging of human breast cancer

Jing Sun[1,2], Zhao-Gang Teng[1], Ying Tian[1], Jian-Dong Wang[1], Yang Guo[2], Dong-Hyun Kim[2], Andrew C Larson[1,2,3,4], Guang-Ming Lu[1]

[1]Department of Medical Imaging, Jinling Hospital, School of Medicine, Nanjing University, Nanjing 210002, China; [2]Department of Radiology, Northwestern University, Chicago, IL 60611, USA; [3]Robert H. Lurie Comprehensive Cancer Center, Chicago, IL 60611, USA; [4]Department of Biomedical Engineering, Northwestern University, Evanston, IL 60208, USA

Received September 23, 2014; Accepted November 25, 2014; Epub December 15, 2014; Published December 30, 2014

Abstract: Magnetic nanoclusters coated with ruthenium (II) complexes doped with silica (fluorescent magnetic nanoparticles or FMNPs) could be used for magnetic resonance imaging (MRI) and optical imaging (OI) of human breast cancer. To achieve the targeting imaging of tumors, the peptide cyclic-arginine-glycine-aspartic acid (RGD) was chosen as the probe for specific targeting integrin $\alpha_v\beta_3$ over expressed in human breast cancer MDA-MB-231 cells. The cytotoxicity tests *in vitro* showed little toxicity of the synthesized RGD-FMNPs with the size of 150 nm. The *in vivo* study also showed no obvious acute toxicity after the injection of RGD-FMNPs in mice bearing MDA-MB-231 tumors. After 24 hours of co-culture with MDA-MB-231 cells, the cellular uptake of RGD-FMNPs significantly increased compared to that of FMNPs. T_2-weighted (T_2W) MRI demonstrated a negative enhancement in mice injected with RGD-FMNPs approximately three times of that injected with FMNPs (12.867 ± 0.451 ms vs. 4.833 ± 0.513 ms, $P < 0.05$). The Prussian blue staining results confirmed more RGD-FMNPs accumulated around the tumors than FMNPs. These results demonstrated the potential application of RGD-FMNPs as a targeting molecular probe for detection of breast cancer using MRI and OI. The synthesized RGD-FMNPs could be potentially used for biomedical imaging in the future.

Keywords: Fluorescent magnetic nanoparticles (FMNPs), magnetic resonance imaging (MRI), optical imaging (OI), ruthenium complexes, RGD, breast cancer

Introduction

Breast cancer is the most common cancer of women except for skin cancer, and it has become the second leading cause of cancer deaths in women cancers [1]. The most efficient way to reduce breast cancer mortality and morbidity is early detection and diagnosis. Thus, it is important to develop a noninvasive imaging method for the early diagnosis of breast cancer.

Owing to the unique magnetic features and important applications in biomedicine and therapeutics, magnetic nanoparticles (MNPs) have attracted much attention during the past few decades. Among the various magnetic materials, superparamagnetic iron oxides (SPIOs) have been considered as ideal candidates for biological applications due to their superparamagnetism, high saturation magnetization and rapid magnetic response to the external magnetic field. For example, SPIOs have been widely used as contrast agents for noninvasive magnetic resonance imaging (MRI). In order to enhance the sensitivity of MRI, great efforts have been made to increase the relaxivity of SPIOs by increasing the particle size [2]. However, there is a superparamagnetic to ferromagnetic transition with increasing particle sizes. Thus, the large ferromagnetic particles easily aggregate in physiological environments [3, 4]. Recently, it is found that magnetic nanoclusters (MNCs) composed of multiple small MNPs can retain the superparamagnetic characters and simultaneously, the transverse relaxivity increases noticeably with the increasing sizes of MNCs [5-11]. This phenomenon pro-

vides great potential of MNCs for their applications in MRI.

Besides the magnetic properties, the biocompatibility of magnetic materials is very important for clinical applications. Although iron is an element of the human body, the high local concentration of iron cations caused by degradation of SPIOs is still toxic to organisms. On the other hand, the aggregation of MNCs in physiological environments is also a big problem that limits their application in the biomedical field. Surface coating can not only prevent iron leaching in biological environments, but also improves the dispersibility of MNCs in solution. Silica has been used as an ideal material to coat various metal oxides because of its excellent biocompatibility and abundant Si-OH active bonds. However, the silica shell in these works is generally used as a protecting layer; especially, the silica coating on MNCs with fluorescent properties are rarely reported. The ruthenium (II) complexes can be doped into the silica coating to form a fluorescent shell for optical imaging. Thence the fluorescent silica coating can combine with the magnetic properties of MNCs, which are termed fluorescent magnetic nanoparticles (FMNPs), to allow both OI and MRI. The ruthenium (II) complexes would be doped into the silica shell as a constituent part of the fluorescent shell to avoid quenching due to the aggregation of fluorescent molecules [12-14]. Definitely, magnetic fluorescent particles can not only be used for MRI but also for optical imaging, thus providing great promise for tumor detection.

Targeting is another issue needs to be considered for imaging. To achieve this aim, various biological molecules such as proteins, antibodies, peptides, and oligo-nucleotides have been demonstrated as targeting molecules. As an important finding, RGD peptide (arginine-glycine-aspartic acid) can selectively combine with the integrin $\alpha_v\beta_3$ which is over expressed in several types of malignancies such as breast cancer, glioblastoma, prostate carcinoma, and pancreatic tumors [15-17]. The integrin is associated with the tumor progression, invasion, and metastasis. So the over-expression in tumor tissues makes it an appealing target site for imaging and therapy [18-21]. Integrin $\alpha_v\beta_3$ has been proven to be over expressed in breast carcinoma and has been utilized as a targeted site for imaging. In this study, cyclic RGD peptides and the highly selective $\alpha_v\beta_3$ integrin ligands were chosen as the targeting probe for breast cancer imaging. The surface of fluorescent silica shell could be easily functionalized with RGD peptides. The RGD peptides would act as the targeting probe and could selectively combine with the integrin $\alpha_v\beta_3$ over expressed in the human breast cancer cell line MDA-MB-231.

In this study, a dual-modality contrast agent is developed for specifically targeting imaging of breast tumors. The magnetic core was composed of MNCs, which could be detected at a low concentration due to their high transverse relaxivity values. The fluorescent silica shell doped with ruthenium (II) complexes would combine OI with MRI to form a contrast agent for dual-modality imaging. To achieve the targeting imaging of human breast cancer, the RGD peptide was chosen as the molecular probe. The targeting imaging of human breast cancer would be achieved through the targeting combination of the RGD peptide with the integrin $\alpha_v\beta_3$. The characterization and biocompatibility of these particles would be evaluated both *in vitro* and *in vivo*. The feasibility of RGD-FMNPs applications would also be evaluated in this study.

Material and methods

Materials

The chemicals iron (III) chloride ($FeCl_3$), sodium acrylate (CH_2 = CHCOONa), sodium acetate (NaOAC), ethylene glycol (EG), diethylene glycol (DEG), dichlorotris (1, 10-phenanthroline) ruthenium (II) hydrate, ethanol (EtOH, 99.5%), concentrated ammonia aqueous solution (25%, wt), tetraethyl orthosilicate (TEOS), and (3-Aminopropyl) triethoxysilane (APTES) were purchased from Sigma-Aldrich (St. Louis, MO, US) and used without further purification. Cyclo (RGDyE) was provided by GL Biochem Ltd. (Shanghai, P.R. China). The cell counting kit-8 (CCK-8) was purchased from Keygen Biotech. Co., Ltd. (Nanjing, Jiangsu, P.R. China).

Synthesis of fluorescent magnetic nanoparticles (FMNPs)

The MNCs composed of Fe_3O_4 nanoparticles were synthesized by the hydrothermal reaction referring to a previously reported protocol [22]. Briefly, $FeCl_3$ (0.325 g), sodium acrylate (1.500

g) and sodium acetate (1.500 g) were dissolved in a mixture of EG (5.0 ml) and DEG (15.0 ml) under magnetic stirring. Then, the homogenous solution was transferred to a Teflon-lined stainless steel autoclave. The autoclave was sealed and heated to 200°C. After reacting for 10 hours, the obtained products were washed five times with ethanol and water. To synthesize the FMNPs, MNCs (1.300 mg) were dispersed in an ethanol aqueous solution (50.0 ml) containing concentrated ammonia aqueous solution (1.7 ml, 25 wt %) and water (1.0 ml), following by the addition of 0.3 ml of TEOS. After the mixture was stirred at 40°C for three hours, $Ru(Phen)_3^{2+}$ ethanol solution (3.0 ml, 0.1 mg/ml) was added, as recommended by the literature [14]. The reaction continued for another three hours, and the obtained products were collected and washed three times with ethanol and water. The obtained particles were dispersed in water.

Functionalization of FMNPs

To form the RGD-FMNPs, (3-aminopropyl) triethoxysilane (APTES) was used as a coupling agent to attach cyclo (RGDyE) to the surface of the FMNPs [23, 24]. The APTES-RGD was first prepared by dissolving RGD (3.000 mg) in a mixture solution of APTES (20.0 μl) and EtOH (1.0 ml) and was allowed to react for 24 hours in the dark. The FMNPs (10.000 mg) were dispersed into the obtained solution (0.5 ml) and kept in dark to react for additional 24 hours. The obtained products were washed three times with ethanol and water, and then were dispersed into PBS.

Characterization of FMNPs

TEM images were taken on JEOL JEM-2100 electronic microscope at 200 kV. X-ray diffraction (XRD) patterns were obtained with a Bruker D8 focus diffractometer. The data were collected at a wavelength of 0.154 nm (40 kV, 40 mA) and a continuous scan mode from 15.00° to 75.00° with the sampling interval of 0.02°. The relaxivity of magnetic particles were assessed through MRI. The phantoms were prepared by dispersing nanoparticles containing different concentrations of iron (0.0000, 0.0893, 0.1786, 0.2679, 0.3572, and 0.4465 mM) in 1% agarose gel and scanned with a clinical 3T MRI scanner (TIM Trio, Siemens). Images were acquired with a T_2-weighted multi-echo [eight time echoes (TEs) ranging from 14.9 ms to 119.2 ms], fast spin-echo sequence [Time Relaxation (TR) = 1,850 ms, slice thickness = 1.5 mm]. The T_2 values were measured through drawing regions of interest (ROIs) on T_2 maps. The conjugation of RGD to the surface of FMNPs was confirmed by Fourier transform infrared (FTIR) spectra (Shimadzu IRPrestige-21 spectrophotometer).

Cell culture and cytotoxicity in vitro

The human breast cancer cell line MDA-MB-231 (ATCC, MD, USA) were cultured in L-15 medium (Gibco, Invitrogen Co., Grand Island, NY, US) supplemented with 10% FBS and 1% penicillin-streptomycin solution at 37°C with 5% CO_2 and 95% humidity. The cytotoxicity *in vitro* was determined by using the CCK-8 assay. Briefly, MDA-MB-231 cells were seeded into 96-well plates at a concentration of 10^4 cells per well. After 24 hours of incubation, the medium was removed and fresh medium with different concentrations (0, 20, 40, 60, 80, 100, 120, 140, 160, 180, and 200 μg/ml) of FMNPs and RGD-FMNPs were added into the wells. Five replicates were run for each concentration. After an additional 24 hours of incubation, the medium was removed, and the cells were rinsed three times with PBS. Then 200 μl of fresh medium with 10 μl of CCK-8 solution was added to each well and incubated with the cells at 37°C, 5% CO_2 for four hours. The OD values were measured at wavelength of 450 nm (A_{450}). The cell viability of untreated group of cells was assumed to be 100%. The cell viabilities of cells treated with FMNPs and RGD-FMNPs were calculated by the following formula:

Cell viability (100%) = [(Ā sample - Ā blank)/(Ā control - Ā blank)] × 100%.

In vitro cellular uptake of RGD-FMNPs

MDA-MB-231 cells were seeded into six well plates with L-15 medium. After 24 hours of incubation, the medium was removed, and then fresh medium containing either FMNPs or RGD-FMNPs (100 μg/ml) was added into each well. The plates were placed in the incubator for an additional 24 hours to allow the particles to interact with the cells. Three wells of cells were harvested and fixed for TEM. The other three wells were used for Prussian blue staining. All the liquid in three wells was removed by aspiration, and the cells were rinsed three times with

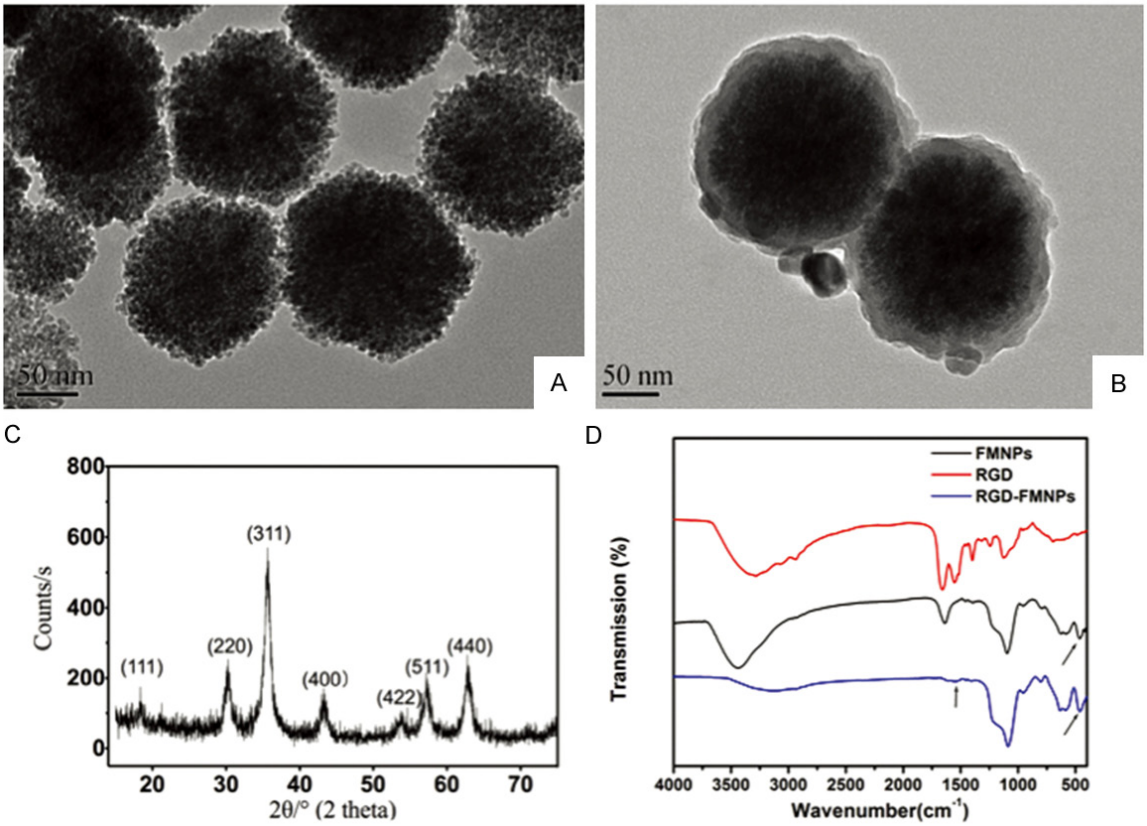

Figure 1. TEM images of the uniform sizes and shapes of MNCs (A) and FMNPs (B); XRD pattern of the small crystallite size of the Fe_3O_4 nanoparticles (C); FTIR spectra of RGD-FMNPs indicate the conjugation RGD peptide onto the FMNPs (D).

1 × PBS. The cells were then fixed with 4% paraformaldehyde at room temperature. After 15 minutes, each well was rinsed three times with 1 × PBS. The cells were stained with Prussian blue and observed with an optical microscope.

In vivo MRI and acute toxicity in vivo

This study was performed according to the animal care guideline of China. All protocols were approved by our Institutional Animal Care and Ethics Committee of Jinling Hospital (Permit Number: 2009449). The BALB-C nude mice (female, 4 to 5 weeks old and 20.0 ± 2.0 g) were obtained from the Comparative Medicine Center of the hospital. A total of 10^6 MDA-MB-231 cells dispersed in 100 μl of PBS were injected into the right side of each mouse. A MR scan was performed on a clinical 3T MRI scanner (TIM Trio, Siemens Medical Solutions, Erlangen, Germany) three weeks after the implantation. 12 mice were divided into two equal groups randomly. One group was injected with FMNPs and the other group was injected with RGD-FMNPs (10 mg/kg in 200 μl PBS) via the tail vein. MRI examinations were performed at pre-injection and six hours after the injections. After the MRI examinations, the mice were euthanized, and the tumors were dissected for Hematoxylin/Ensin (HE) and Prussian blue staining. Additional groups of mice (each group n = 6) were used for the acute toxicity tests. The mice received RGD-FMNPs at doses of 5.0, 10.0, and 20.0 mg/kg in 200 μl PBS via the tail vein. The control group received 200 μl PBS injections. Animals were observed for events indicative of acute toxicity, i.e., vital signs, behavior, diet, and activity level, following administration of the probe for 96 hours.

Data analysis and statistics

The post-processing of MR images was performed by using software Matlab (MathWorks, Natick, MA). Regions of interest (ROIs) were drawn manually on T_2-weighted images to encompass the tumor regions for T_2 value calculation. The results were shown as mean ±

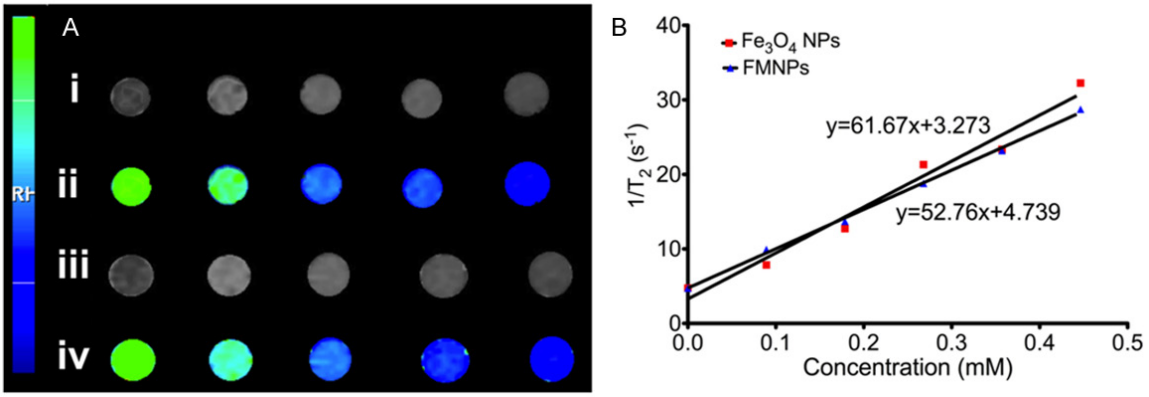

Figure 2. Magnetic properties of the synthesized nanoparticles. (A) MRI images of phantoms of MNCs (i and ii) and FMNPs (iii and iv) containing increasing concentrations of iron (from left to the right, the concentrations were 0, 0.0893, 0.1786, 0.2679, 0.3572, and 0.4465 mM respectively. The concentrations were same for each column). The relaxivities of FMNPs and MNCs were 52.76 mM^{-1} s^{-1} (A) and 61.67 mM^{-1} s^{-1} (B) respectively.

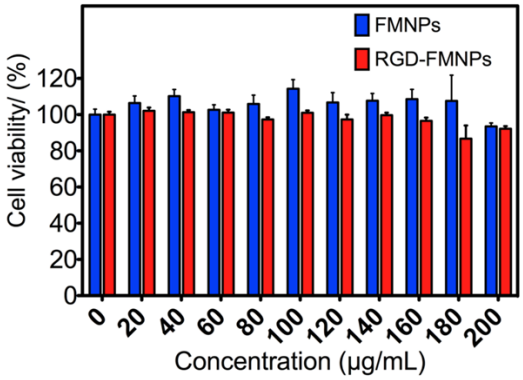

Figure 3. Cytotoxicity analysis results with the MTT assay. The viability of human breast cancer MDA-MB-231 cells after 24 hours of incubation with different concentrations (0, 20, 40, 60, 80, 100, 120, 140, 160, 180, and 200 μg/ml) of FMNPs and RGD-FMNPs remained above 90%.

standard deviation. Student's t test was used to compare the differences in decreases of T_2 values between groups. $P < 0.05$ was considered to be statistically significant for all the analysis.

Results

Characterization of FMNPs

The TEM images indicated that the average size of MNCs was approximately 100 nm. The MNCs are composed of small nanoparticles with a size of about 10 nm. Both the MNCs and the FMNPs were very uniform in sizes and shapes (**Figure 1A**, **1B**). The fluorescent silica shell is about 20 to 30 nm, and the size of FMNPs is 150 nm. XRD (**Figure 1C**) result shows sites and intensities of the diffraction peaks are consistent with the standard pattern for JCPDS Card No. (79-0417). The samples showed very broad peaks, indicating the ultra-fine nature and small crystallite size of MNPs. According to the Debye-Scherrer formula, the particle size was determined to be 10 nm by taking the average of the sizes at the peaks (D220, D311, D400, D422, D511 and D440 respectively). The conjugation of RGD peptides was confirmed via Fourier transform infrared (FTIR-spectra) analysis, which is shown in **Figure 1D**. Characteristic bands of Amide I and II bands at ~1,550 cm^{-1} and 1,670 cm^{-1} were observed on the spectrum of RGD-FMNPs, which indicate the presence of associated peptide bonds on the surface of the FMNPs. In addition, N-H stretching ~3,200 cm^{-1} of RGD peptide was characterized. The transverse relaxivity of the particles was measured through the MRI. The T_2-weighted images of phantoms with different concentrations of MNCs (**Figure 2A** i and ii) and FMNPs (**Figure 2A** iii and iv) showed decreased signal intensity with the increasing iron concentration (0, 0.0893, 0.1786, 0.2679, 0.3572, and 0.4465 mM). The r_2 value of MNCs was and FMNPs were 52.76 mM^{-1} s^{-1}, 61.67 mM^{-1} s^{-1} respectively (**Figure 2B**).

Cytotoxicity in vitro and acute toxicity in vivo

The biocompatibility of nanoparticles is one of most important characters for biomedical application. Thus, a cytotoxicity experiment *in vitro* and acute toxicity test *in vivo* were done to

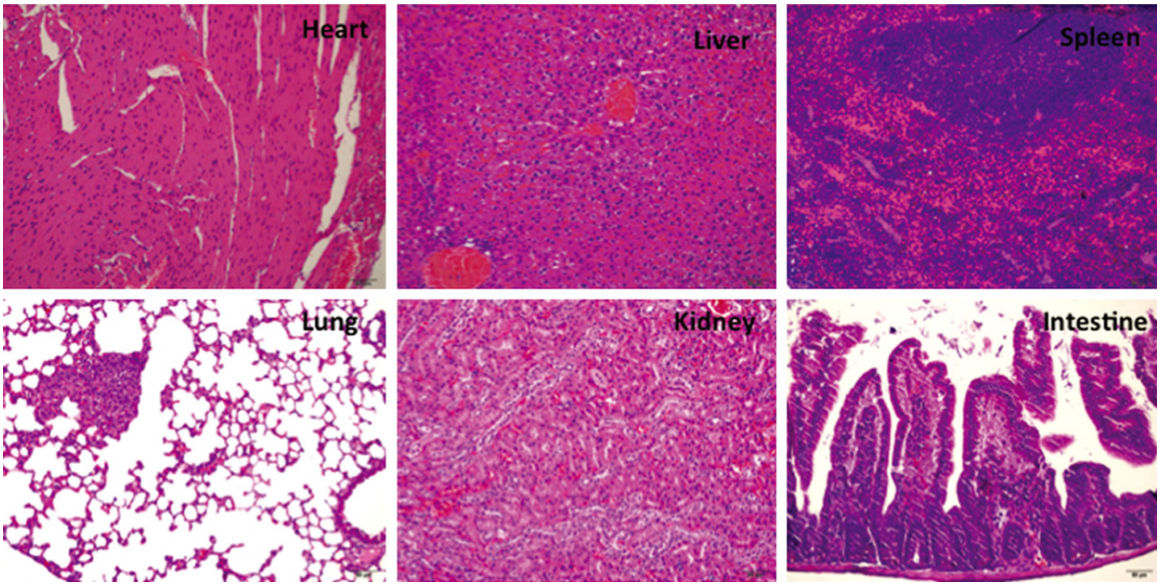

Figure 4. HE staining results of representative tissue sections of mice (heart, liver, spleen, lung, kidney, and intestine) after injection of RGD-FMNPs. No obvious pathological changes were observed in the different tissues.

evaluate the biocompatibility of the synthesized RGD-FMNPs. The cell viabilities after incubation with different concentrations (0, 20, 40, 60, 80, 100, 120, 140, 160, 180, 200 μg/ml) of FMNPs and RGD-FMNPs were evaluated by using the CCK-8 assay (**Figure 3**). There was little cytotoxicity observed in the cells incubated with FMNPs. For the cells treated with RGD-FMNPs, the cell viability was a little lower compared to that of cells treated with the same concentrations of FMNPs. However, the cell viability remained above 90% even when treated at the concentration of 200 μg/ml. Acute toxicity tests were performed *in vivo*: all mice survived and no abnormal reactions were observed in vital signs, behavioral status, diet, or activity levels 96 hours after the administration of RGD-FMNPs. The acute toxicity *in vivo* was also evaluated through histological assessment. The representative organs (heart, liver, spleen, lung, kidney and intestine) were harvested at six hours after the injection of RGD-FMNPs. The HE staining results (**Figure 4**) appear normal in the different organs. There were no obvious acute toxicities observed in any organs.

Cellular uptake in vitro

The cellular uptakes of FMNPs and RGD-FMNPs were confirmed through fluorescent microscopy, TEM, and Prussian blue staining (**Figures 5**, **6**). Both FMNPs and RGD-FMNPs were able to enter into the human breast cancer MDA-MB-231 cells. However, more RGD-FMNPs were taken into the cells compared to FMNPs. The fluorescent intensity of the particles taken into cells was analyzed through the software Image J (National Institutes of Health, MD, USA). The fluorescent intensity of RGD-FMNPs (**Figure 5E**, **5F**) was higher than that of FMNPs (**Figure 5B**, **5C**). The arrows in **Figure 6A**, **6B** indicate the presence of both particles in MDA-MB-231 cells. Prussian blue staining results also confirmed the cellular uptake of FMNPs and RGD-FMNPs. There was an enhanced cellular uptake of the RGD-FMNPs (**Figure 6D**) compared to the FMNPs (**Figure 6C**).

MRI in vivo

A MRI was performed to evaluate the application of RGD-FMNPs as a targeting imaging contrast agent. T_2-weighed images were taken before and after the injection of FMNPs and RGD-FMNPs (**Figure 7**). The T_2 values in the tumor regions decreased six hours after injection (**Figure 7B**, **7E**) compared to baseline images before the injection of the FMNPs (**Figure 7A**) or RGD-FMNPs (**Figure 7D**). Differences were found in the decreases of T_2 values after the injection of FMNPs and RGD-FMNPs (4.833 ± 0.513 ms vs. 12.867 ± 0.451 ms, $P < 0.05$). The representative T_2 maps were shown in **Figure 7** (ΔT_2 = 3.327 ms vs. 11.439 ms). Prussian blue staining results showed the exis-

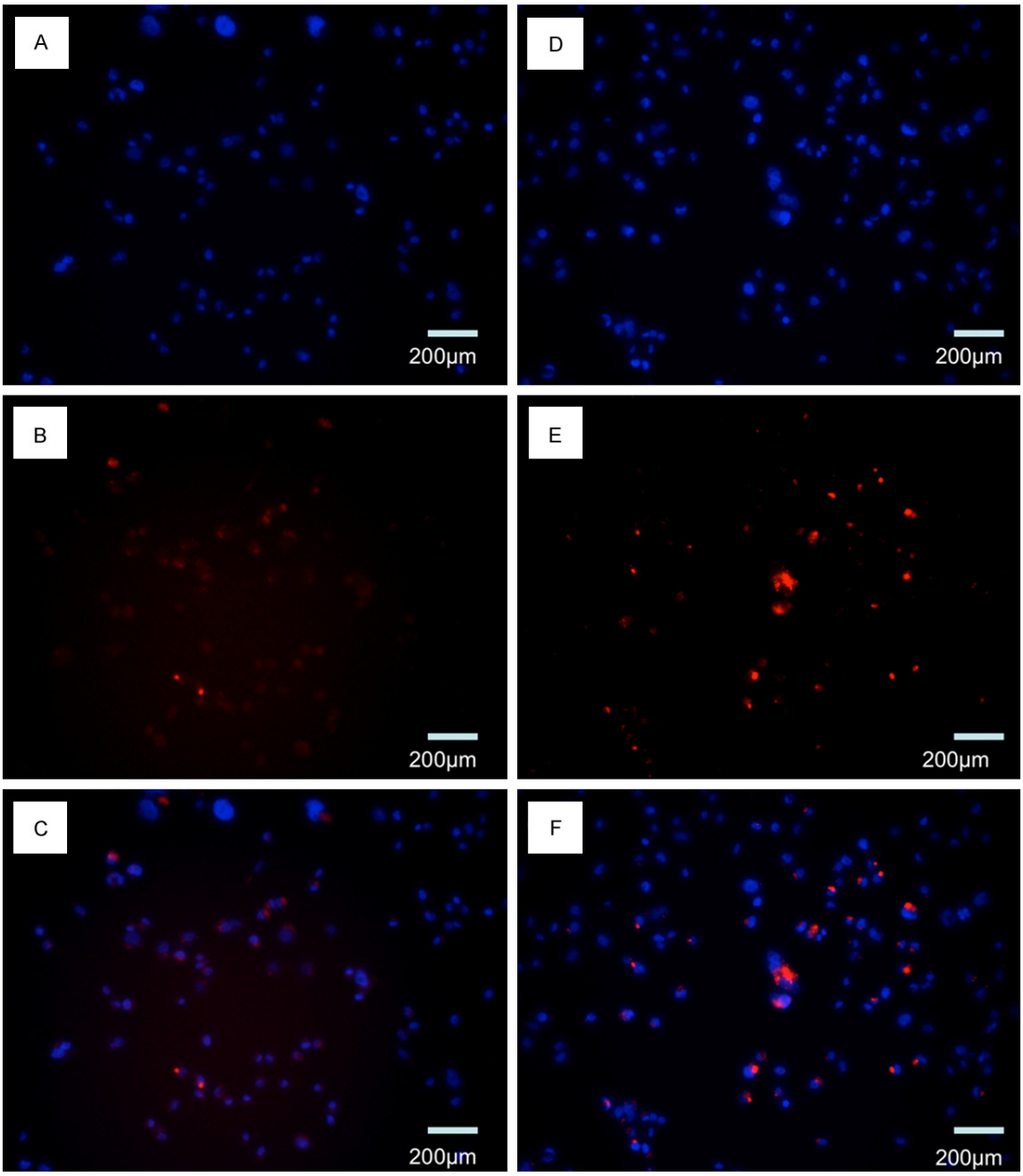

Figure 5. Fluorescent microscopy results of cellular uptake of FMNPs (A-C) and RGD-FMNPs (D-F). The nuclear was stained with DAPI (A, D) and the red color represents the Ru (II) doped in silica shell (B, E). The combined images were shown in (C, F). Both particles can be taken into MDA-MB-231 cells (B, E). The fluorescent intensity of RGD-FMNPs (E, F) was higher than that of FMNPs (B, C) through the quantitative analysis with software of Image J.

tence of RGD-FMNPs and FMNPs in tumors (**Figure 7C**, **7F**).

Discussion

In this study, a potential dual-modality targeting imaging contrast agent (RGD-FMNPs) was introduced. It was conjugated with a specific targeting probe cyclo (RGDyE), which can recognize integrin $\alpha_v\beta_3$ over expressed on human breast cancer cells. These RGD-FMNPs possess magnetic and fluorescent properties, which can be used for both MRI and OI. The targeting probe RGD peptides could enhance the accumulation

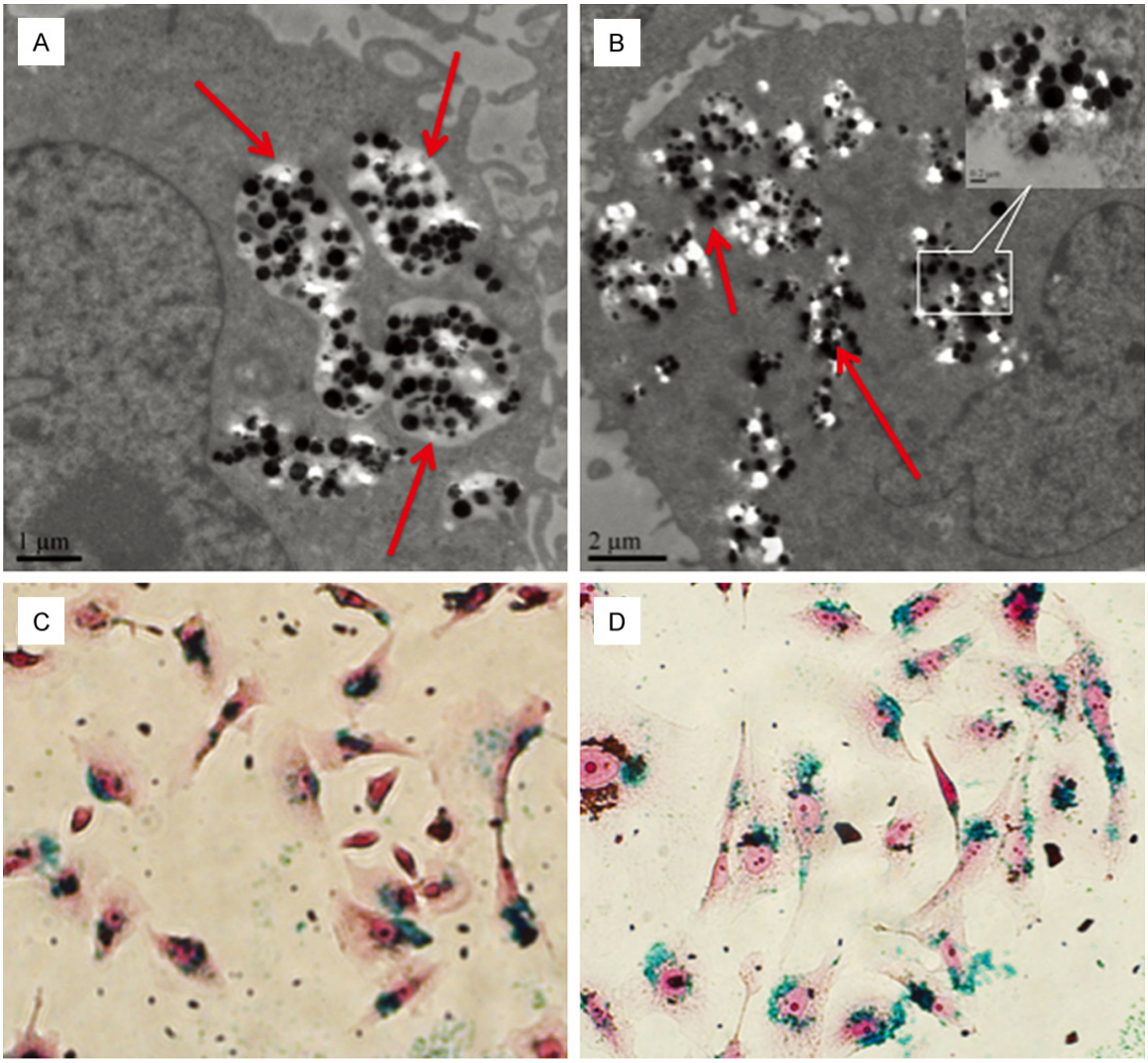

Figure 6. Cellular uptakes of FMNPs and RGD-FMNPs. TEM images showing cellular uptake of FMNPs (A) and RGD-FMNPs (B) by human breast cancer MDA-MB-231 cells. The arrows indicate the presence of nanoparticles in MDA-MB-231 cells. The upper-right corner of (B) shows the magnified of RGD-FMNPs in MDA-MB-231 cells. Prussian blue staining results also confirmed the cellular uptake of FMNPs (C) and RGD-FMNPs (D) by MDA-MB-231 cells.

of the particles in tumor cells for cancer diagnosis.

The highly water soluble MNCs were synthesized using a one-step hydrothermal method [22]. Large amounts of carboxyl groups (-COOH) present on Fe_3O_4 surface, which render these nanoclusters very soluble in water and can be used as templates for well defined core/shell structures. These MNCs maintain the superparamagnetism and high transverse relaxivity. Due to the high magnetization, they could be detected at a low concentration and could be used as negative T_2W or T_2^*W MRI contrast agents. The MRI phantom studies showed the high r_2 values of MNCs and FMNPs. Even at very low concentration of FMNPs, the decrease of T_2WI signal intensity was evident with increasing TEs, which indicated FMNPs could be potentially used as MRI contrast agents.

Silica is widely used for fluorescent dye doping because it allows emission and excitation photons to be transmitted without any alterations, which can be used as the coating of various fluorescence materials [25-28]. In addition, silica is highly water-soluble and has good biocompatibility [29]. The cytotoxicity study *in vitro* demonstrated that there was little toxicity after coating with a silica shell. The cell viability

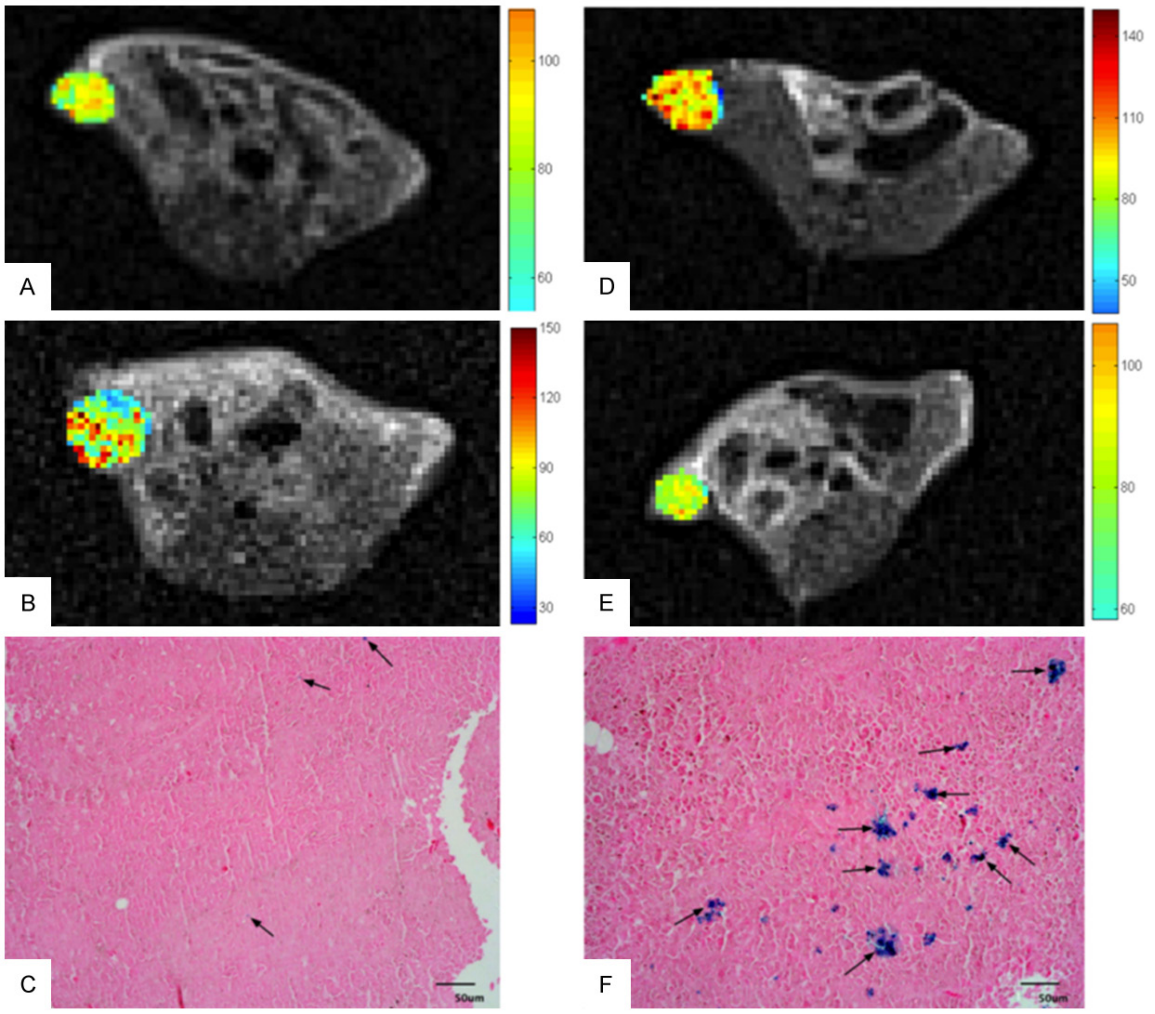

Figure 7. *In vivo* MRI images of mice and Prussian blue staining results of tumors. MR scans were performed before the injection as the baseline images (A, D) and post-scans (B, E) were performed at six hours after injection of FMNPs (A, B) and RGD-FMNPs (D, E) via tail vein. The Prussian blue staining results of tumors were shown (C, F) to confirm the existence of iron.

remained above 90% even at the highest concentration (200 μg/ml). The fluorescent dye Ru (II) was doped into the silica shell to form a fluorescent shell, which could be used for OI. The spherical surface of silica-coated particles could be easily functionalized with various targeting molecules. The fluorescent microscopy, TEM and Prussian blue staining results indicated that both the FMNPs and RGD-FMNPs could be taken into the MDA-MB-231 cells through endocytosis. RGD peptides, which act as targeting probes, can recognize and specifically bind to integrin $\alpha_v\beta_3$ which is over expressed in MDA-MB-231 cells. Due to the targeting role of RGD peptides, more RGD-MNPs would target the MDA-MB-231 cells and the uptake of RGD-MNPs was enhanced compared to that of FMNPs. Therefore it was RGD peptides that enhanced the cellular uptake of RGD-FMNPs. The cytotoxicity *in vitro* was also evaluated. Compared to FMNPs, the cell viability was a little lower at the same concentration. This may be caused by the enhanced uptake of RGD-FMNPs due to the targeting effect of the RGD peptides. However, even at the highest concentration of 200 μg/ml, the cell viability was still above 90%. This result indicated little cytotoxicity of the synthesized RGD-FMNPs and a great potential of application of *in vivo* tumor imaging. The HE results of the representative organs also showed little obvious acute toxicity after the injection of either FMNPs or RGD-FMNPs. The different organs, including the heart, liver, spleen, lungs and kidneys, were harvested six

hours after the injection of the particles. There were no obvious pathological changes in any organs. No inflammatory reactions or necrosis were observed in liver. The spleen also seemed normal. There were no inflammatory nodules or any acute injury in the lungs or other organs. Also, no obvious degeneration or necroses were observed in any of the organs. These findings indicated that the synthesized nanoparticles exhibited little toxicity and could be used for biomedical imaging in future. All of these results indicated the potential application of RGD-FMNPs as an imaging agent in the biomedical field.

The T_2-weighted MR images *in vivo* demonstrated the signal intensity decreased in the tumor region after the injection of FMNPs and RGD-FMNPs. T_2 maps also demonstrated the decreased T_2 values of tumor regions. The decreases of T_2 values were much more notable in the tumors of mice injected with RGD-FMNPs compared to those with FMNPs (12.867 ± 0.451 ms vs. 4.833 ± 0.513 ms; $P < 0.05$). This result is due to the tumor targeting function of the RGD peptides. The RGD peptide could bind with the integrin $\alpha_v\beta_3$ expressed both on the tumor cells and endothelial cells. Then, the RGD-FMNPs would be internalized through the receptor-mediated endocytosis [30, 31]. The EPR effect combined with the acting targeting effect of RGD peptides would increase the accumulation of the RGD-FMNPs in the tumors, which thus led to the decreases of T_2 values in the tumor regions. These decreases were also consistent with the results of the Prussian blue staining of the tumors (**Figure 7C**, **7F**). These results indicate that the RGD-FMNPs could be used as a MRI contrast agent for detecting tumors in which the integrin $\alpha_v\beta_3$ is highly expressed. Integrin $\alpha_v\beta_3$ is over expressed not only human breast cancer, but also many other malignant tumors such as melanoma, prostate, pancreatic, ovarian, cervical, glioblastoma, lung and colon cancer [32]. Therefore, these RGD-FMNPs can potentially be used for improved targeting of a very wide range of cancer types.

There were also some limitations in this study. The maximum emission peak of the Ru (II) doped silica nanoparticles was approximately 588 nm at an excitation wavelength of 450 nm. This may limit the application of imaging of orthotopic tumors and deep organs. So introduction of another near-infrared dye will be tried in a future study to improve this. However, these RGD-FMNPs could still be used to quickly identify the intra-operative boundary of tumors via pathologic analysis or to determine whether there are lymph nodes metastases. For real-time optical imaging *in vivo*, it is better to use the near-infrared fluorescent dyes, which have penetration depths of up to a couple of centimeters. Therefore, in the future, studies will focus on the near-infrared fluorescent dyes and try to develop simultaneous real-time imaging nanoparticles for both MRI and OI.

Conclusion

The synthesized RGD-FMNPs can be used for targeting imaging of breast cancer through MRI and OI. The conjugated RGD peptides can enhance the cellular uptake in human breast cancer MDA-MB-231 cells. This study shows the potential application of RGD-FMNPs to be used in biomedical targeting imaging in the future.

Acknowledgements

The authors report no conflicts of interest in this work. Grant Support for this work was supported by the National Key Basic Research Program of the People's Republic of China (2014CB744500 and 2011CB707700), the Major International (Regional) Joint Research Program of China (81120108013), and the National Science Foundation of China (NSFC) (30930028, 81101039, 81322020, 81230032, 81371611 and 81171313). We are also thankful for the financial support of the China Scholarship Council (CSC).

Disclosure of conflict of interest

None.

Address correspondence to: Dr. Guang-Ming Lu, Department of Medical Imaging, Jinling Hospital, School of Medicine, Nanjing University, 305 East Zhongshan Road, Nanjing 210002, P.R. China. Tel: +86-25-8086-0185; Fax: +86-25-8480-4659; E-mail: cjr.luguangming@vip.163.com

References

[1] Desantis C, Ma J, Bryan L and Jemal A. Breast cancer statistics, 2013. CA Cancer J Clin 2014; 64: 52-62.

[2] Roca AG, Marco JF, Morales MdP and Serna CJ. Effect of nature and particle size on properties of uniform magnetite and maghemite nanoparticles. J Phys Chem C 2007; 111: 18577-18584.
[3] Deng H, Li X, Peng Q, Wang X, Chen J and Li Y. Monodisperse magnetic single-crystal ferrite microspheres. Angew Chem Int Ed Engl 2005; 44: 2782-2785.
[4] Zhong LS, Hu JS, Liang HP, Cao AM, Song WG and Wan LJ. Self-assembled 3D flowerlike iron oxide nanostructures and their application in water treatment. Adv Mater 2006; 18: 2426-2431.
[5] Berret JF, Schonbeck N, Gazeau F, El Kharrat D, Sandre O, Vacher A and Airiau M. Controlled clustering of superparamagnetic nanoparticles using block copolymers: design of new contrast agents for magnetic resonance imaging. J Am Chem Soc 2006; 128: 1755-1761.
[6] Ge J, Hu Y and Yin Y. Highly Tunable Superparamagnetic Colloidal Photonic Crystals. Angewandte Chemie 2007; 119: 7572-7575.
[7] Ge J, Kwon S and Yin Y. Niche applications of magnetically responsive photonic structures. J Mater Chem 2010; 20: 5777-5784.
[8] Jianping G and Yin Y. Magnetically responsive colloidal photonic crystals. J Mater Chem 2008; 18: 5041.
[9] Ge J, Hu Y, Zhang T, Yin Y. Superparamagnetic Composite Colloids with Anisotropic Structures. Am Chem Soc 2007; 129: 8974-8975.
[10] Ge J, Hu Y, Zhang T, Huynh T, Yin Y. Self-assembly and field-responsive optical diffractions of superparamagnetic colloids. Langmuir 2008; 24: 3671-3680.
[11] Xu F, Cheng C, Xu F, Zhang C, Xu H, Xie X, Yin D and Gu H. Superparamagnetic magnetite nanocrystal clusters: a sensitive tool for MR cellular imaging. Nanotechnology 2009; 20: 405102.
[12] Basabe-Desmonts L, Reinhoudt DN and Crego-Calama M. Design of fluorescent materials for chemical sensing. Chem Soc Rev 2007; 36: 993-1017.
[13] Burns A, Ow H and Wiesner U. Fluorescent core-shell silica nanoparticles: towards "Lab on a Particle" architectures for nanobiotechnology. Chem Soc Rev 2006; 35: 1028-1042.
[14] Zhang D, Wu Z, Xu J, Liang J, Li J and Yang W. Tuning the emission properties of Ru(phen)3(2+) doped silica nanoparticles by changing the addition time of the dye during the Stober process. Langmuir 2010; 26: 6657-6662.
[15] Sheldrake HM and Patterson LH. Function and antagonism of beta3 integrins in the development of cancer therapy. Curr Cancer Drug Targets 2009; 9: 519-540.
[16] Takayama S, Ishii S, Ikeda T, Masamura S, Doi M and Kitajima M. The relationship between bone metastasis from human breast cancer and integrin alpha(v)beta3 expression. Anticancer Res 2005; 25: 79-83.
[17] Vellon L, Menendez JA, Liu H and Lupu R. Up-regulation of alphavbeta 3 integrin expression is a novel molecular response to chemotherapy-induced cell damage in a heregulin-dependent manner. Differentiation 2007; 75: 819-830.
[18] Hersey P, Sosman J, O'Day S, Richards J, Bedikian A, Gonzalez R, Sharfman W, Weber R, Logan T, Lawson D, Zhang J, Hammershaimb L and Kirkwood JM. A phase II, randomized, open-label study evaluating the antitumor activity of MEDI-522, a humanized monoclonal antibody directed against the human alpha v beta 3 (avb3) integrin, +/- dacarbazine (DTIC) in patients with metastatic melanoma (MM). J Immunother 2005; 28: 643-644.
[19] Mulgrew K, Kinneer K, Yao XT, Ward BK, Damschroder MM, Walsh B, Mao SY, Gao C, Kiener PA, Coats S, Kinch MS and Tice DA. Direct targeting of alphavbeta3 integrin on tumor cells with a monoclonal antibody, Abegrin. Mol Cancer Ther 2006; 5: 3122-3129.
[20] Murphy EA, Majeti BK, Barnes LA, Makale M, Weis SM, Lutu-Fuga K, Wrasidlo W and Cheresh DA. Nanoparticle-mediated drug delivery to tumor vasculature suppresses metastasis. PNAS 2008; 105: 9343-9348.
[21] Yamada S, Bu XY, Khankaldyyan V, Gonzales-Gomez I, McComb JG and Laug WE. Effect of the angiogenesis inhibitor cilengitide (EMD 121974) on glioblastoma growth in nude mice. Neurosurgery 2006; 59: 1304-1312.
[22] Xuan S, Wang YXJ, Yu JC and Cham-Fai Leung K. Tuning the Grain Size and Particle Size of Superparamagnetic Fe_3O_4 Microparticles. Chem Mater 2009; 21: 5079-5087.
[23] Ebrahiminezhad A, Ghasemi Y, Rasoul-Amini S, Barar J and Davaran S. Preparation of novel magnetic fluorescent nanoparticles using amino acids. Colloids Surf B Biointerfaces 2013; 102: 534-539.
[24] Ferris DP, Lu J, Gothard C, Yanes R, Thomas CR, Olsen JC, Stoddart JF, Tamanoi F and Zink JI. Synthesis of biomolecule-modified mesoporous silica nanoparticles for targeted hydrophobic drug delivery to cancer cells. Small 2011; 7: 1816-1826.
[25] Lee CS, Chang HH, Jung J, Lee NA, Song NW and Chung BH. A novel fluorescent nanoparticle composed of fluorene copolymer core and silica shell with enhanced photostability. Colloids Surf B Biointerfaces 2012; 91: 219-225.
[26] Li Z, Zhang Y and Jiang S. Multicolor Core/Shell-Structured Upconversion Fluorescent

Nanoparticles. Adv Mater 2008; 20: 4765-4769.
[27] Liu X, Qian H, Ji Y, Li Z, Shao Y, Hu Y, Tong G, Li L, Guo W and Guo H. Mesoporous silica-coated NaYF4 nanocrystals: facile synthesis, in vitro bioimaging and photodynamic therapy of cancer cells. RSC Adv 2012; 2: 12263.
[28] Nagarajan S and Zhang Y. Upconversion fluorescent nanoparticles as a potential tool for in-depth imaging. Nanotechnology 2011; 22: 395101.
[29] Chang JS, Chang KL, Hwang DF and Kong ZL. In vitro cytotoxicitiy of silica nanoparticles at high concentrations strongly depends on the metabolic activity type of the cell line. Environ Sci Technol 2007; 41: 2064-2068.
[30] Prokop A and Davidson JM. Nanovehicular intracellular delivery systems. J Pharm Sci 2008; 97: 3518-3590.
[31] Sahay G, Alakhova DY and Kabanov AV. Endocytosis of nanomedicines. J Control Release 2010; 145: 182-195.
[32] Desgrosellier JS and Cheresh DA. Integrins in cancer: biological implications and therapeutic opportunities. Nat Rev Cancer 2010; 10: 9-22.